

FAST TRACK COMMUNICATION • OPEN ACCESS

Size matters for nonlinear (protein) wave patterns

To cite this article: Fabian Bergmann *et al* 2018 *New J. Phys.* **20** 072001

View the [article online](#) for updates and enhancements.

Related content

- [Stochastic switching between multistable oscillation patterns of the Min-system](#)
Artemij Amiranashvili, Nikolas D Schnellbacher and Ulrich S Schwarz
- [Parameter-space topology of models for cell polarity](#)
Philipp Khuc Trong, Ernesto M Nicola, Nathan W Goehring *et al.*
- [Nonlinear self-adapting wave patterns](#)
David A Kessler and Herbert Levine



IOP | ebooks™

Bringing you innovative digital publishing with leading voices to create your essential collection of books in STEM research.

Start exploring the collection - download the first chapter of every title for free.

**FAST TRACK COMMUNICATION**

Size matters for nonlinear (protein) wave patterns

OPEN ACCESSRECEIVED
19 June 2018REVISED
5 July 2018ACCEPTED FOR PUBLICATION
18 July 2018PUBLISHED
27 July 2018Fabian Bergmann¹, Lisa Rapp¹ and Walter Zimmermann

Theoretische Physik I, Universität Bayreuth, D-95440 Bayreuth, Germany

¹ Contributed equally to this work.E-mail: walter.zimmermann@uni-bayreuth.de**Keywords:** pattern formation, biological physics, reaction–diffusion, nonlinear wavesSupplementary material for this article is available [online](#)

Original content from this work may be used under the terms of the [Creative Commons Attribution 3.0 licence](#).

Any further distribution of this work must maintain attribution to the author(s) and the title of the work, journal citation and DOI.

**Abstract**

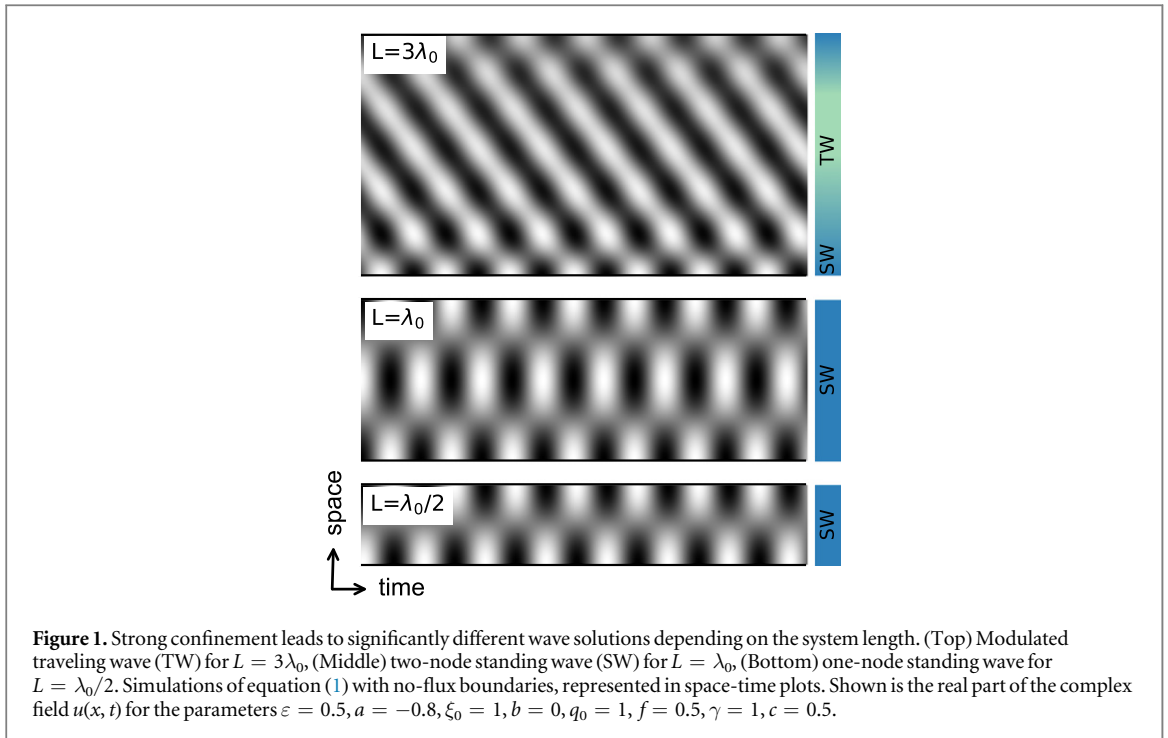
Pattern formation and selection are fundamental, omnipresent principles in nature—from small cells up to geological scales. In *E. coli* bacteria, for example, self-organized pole-to-pole oscillations of Min proteins—resembling a short standing wave—ensure correct positioning of the cell division site. The same biochemical reaction leads to traveling protein waves on extended membranes in *in vitro* experiments. Are these seemingly contradictory observations of system-spanning importance? We show that a transition of nonlinear traveling wave patterns to reflection-induced standing waves in short systems is a generic and robust phenomenon. It results from a competition between two basic phenomena in pattern formation theory. We confirm the generic findings for the cell-biological Min reaction and for a chemical reaction–diffusion system. These standing waves show bistability and adapt to varying system lengths similar as pole-to-pole oscillations in growing *E. coli*. Our generic results highlight key functions of universal principles for pattern formation in nature.

1. Introduction

A variety of fascinating patterns emerges spontaneously in a wealth of living or inanimate driven systems [1–13]. The esthetic appeal of these patterns is immediately apparent to all observers [1]. But universal principles of patterns and their importance in nature also attract researchers from many disciplines. They explore, for instance, the important functions patterns fulfill: self-organized patterns in biology guide size sensing [6], positioning of protein clusters [7], self-driven morphogenesis [8] and communication between species [10]. They furthermore enhance heat transport in fluid systems [3, 11] and are the basis of successful survival strategies for vegetation in water-limited systems [12–14].

Patterns include both stationary spatial structures such as stripes or hexagons, and dynamic structures like traveling waves [1–4]. Traveling waves occur in such different and prominent systems as thermally driven fluid convection [3, 15–18], electroconvection in nematic liquid crystals [19, 20] or the biochemical Min protein reaction on extended membranes [21, 22]. As these examples show, patterns emerge in diverse systems and are driven by very different mechanisms. Nevertheless, once stripes, hexagons or traveling waves have evolved, they often have certain universal properties described by pattern formation theory [2–4, 12].

In nature, patterns often evolve in the presence of domain boundaries—be it the walls of a convection cell, the finite size of a petri dish or the membrane enclosing the cytosol of a biological cell. These boundaries have a strong influence on the process of pattern formation. Stripe patterns, e.g., respond to system boundaries by adjusting their stripe orientation or selecting specific wavelengths [3, 23–25]. System boundaries in general break symmetries. Spatially varying parameters break them, too, and thus have similar effects [26–28]. The response of stationary periodic patterns to such symmetry breaking effects is broadly similar in different systems, i.e. independent of system details [3, 23, 25]. Traveling waves near boundaries show similar fascinating spatio-temporal behavior [15, 16, 29, 30]. However, the effects of strong confinement on nonlinear wave patterns have not yet been thoroughly examined.



In this work, we show that nonlinear traveling waves inevitably change into reflection-induced standing waves in sufficiently short, confined systems. Since this generic phenomenon relies on basic universal principles of pattern formation, we explore it at first within a minimal model for nonlinear traveling waves. The resulting system-spanning properties can then be transferred to related phenomena in nature: in the Min system, e.g., traveling waves form by coordinated attachment and detachment of Min proteins from the membrane. This protein system originates from *E. coli* bacteria where it plays an important role in the cell division process [31–33]: inside the rod-shaped *E. coli* bacteria, oscillating proteins shuttle between the two cell poles. Thereby, they ensure the positioning of the cell division site at the cell center. In *in vitro* experiments on the other hand, the same biochemical reaction leads to traveling waves on large extended membranes [21, 22]. A deeper understanding of generic properties of nonlinear waves in confinement will help to reconcile these seemingly contradictory observations.

2. Transition to reflection-induced standing waves in short systems

We first analyze the transition from nonlinear traveling waves in extended systems to reflection-induced standing waves in strongly confined systems using a generic model. ‘Strong confinement’ refers to short system lengths in the order of the preferred wavelength of the traveling wave. The model we use is the complex Swift–Hohenberg (CSH) model [4, 34–36],

$$\partial_t u(x, t) = (\varepsilon + ia)u - \xi_0^2(1 + ib)(q_0^2 + \partial_x^2)^2 u + if\partial_x^2 u - \gamma(1 + ic)|u|^2 u, \quad (1)$$

for the complex scalar field $u(x, t)$ in one spatial dimension. In extended systems and for $\varepsilon > 0$, this model shows traveling waves with a preferred wavelength $\lambda_0 = 2\pi/q_0$ over a wide range of parameters. We measure the system length L in units of λ_0 since it represents an intrinsic length scale of the problem.

Simulations of equation (1) with no-flux boundary conditions (see appendix A for details) for three different system lengths lead to the results shown in figure 1: depending on the system length, we get three significantly different wave solutions.

In moderately short systems ($L = 3\lambda_0$, top), we find a traveling wave pattern in the center (bulk) of the system. This resembles the traveling wave patterns that occur for the CSH model in large, quasi-unconfined systems. Two traveling wave directions, described by $u_R(x - \omega t)$ (traveling to the right) and $u_L(x + \omega t)$ (traveling to the left), are equally likely in extended pattern forming systems. In contrast to, e.g., light or sound waves, however, traveling waves in pattern forming systems are nonlinear. While light or sound waves are thus superimposable, two counter-propagating nonlinear waves compete with each other: one of the traveling wave directions is spontaneously selected, while the other is suppressed [3, 29]. But their confinement in finite systems introduces an additional effect: traveling waves are reflected at the boundaries of a finite system. The boundary conditions apply to the whole field $u(x, t)$ in equation (1), i.e. the incoming and reflected waves together.

Therefore, the sum $u_R + u_L$, has to match them at the system borders. This boundary coupling forces the incoming and reflected waves into coexistence in a finite neighborhood of the boundary. The resulting superposition of both wave directions leads to standing wave patterns. Further away in the bulk the nonlinear competition between both wave directions dominates and the reflected wave is damped by the predominant incoming traveling wave. The largest system in figure 1 (top) shows the interplay between both bulk and boundary effects. Reflection effects dominate very close to the top and bottom boundaries of the system. There, the incoming and reflected wave form a local standing wave. The extent of this standing wave depends on the distance ε from threshold and increases by decreasing ε . In the bulk region, however, wave competition prevails—the pattern resembles a traveling wave. By decreasing the system length L , the boundaries move closer together, i.e. the fraction of the system with significant superposition of incoming and reflected waves increases. Therefore, the boundary-induced reflection becomes more and more important. For sufficiently short systems—shorter than a critical length L_c —the reflection effect predominates the nonlinear competition in the whole system. As a result, standing waves become inevitable. Note that these standing waves are reflection-induced. In principle, standing wave solutions can be inherently stable. However, this is not the case here: in the CSH model, standing waves in extended systems are always unstable. Thus, the standing waves we find here are a direct consequence of the confinement. While this novel, reflection-induced transition from traveling to standing waves is generic, the critical length L_c depends on the chosen parameters and is specific to each system. The middle and bottom panel in figure 1 show simulations for $L = \lambda_0$ and $L = \lambda_0/2$, respectively. Both system lengths are below L_c leading to standing wave patterns. In the standing wave regime, the system length influences the number of standing wave nodes. For $L = \lambda_0$ (figure 1, middle) and similar lengths, we find a two-node standing wave. If only about half of the preferred wavelength fits into the system (e.g. $L = \lambda_0/2$, figure 1 bottom), the standing wave has a single node in the system center.

3. Length adaptability and bistability of nonlinear standing waves

The discovered reflection-induced standing waves in strongly confined systems are further characterized by exploring their linear stability. For stationary stripe patterns it is well known that they are stable for different wavenumbers in a finite band width. The basis of this multistability is the so-called Eckhaus stability band [37, 38]. Both fluid experiments [39, 40] and numerical analysis of different systems [27, 41] confirmed multistability for stationary patterns (e.g. stripes) in extended systems. The Eckhaus stability band also exists for traveling waves in unconfined systems [4, 17, 42, 43]. Do the standing waves we find in strongly confined systems also show multistable behavior? Does the confinement influence the stability band compared to spatially extended systems?

An analytical approximation of a standing wave solution of equation (1) is given by

$$u(x, t) = Fe^{-i\Omega t}[e^{iqx} + e^{-iqx}] = 2Fe^{-i\Omega t} \cos(qx), \quad (2)$$

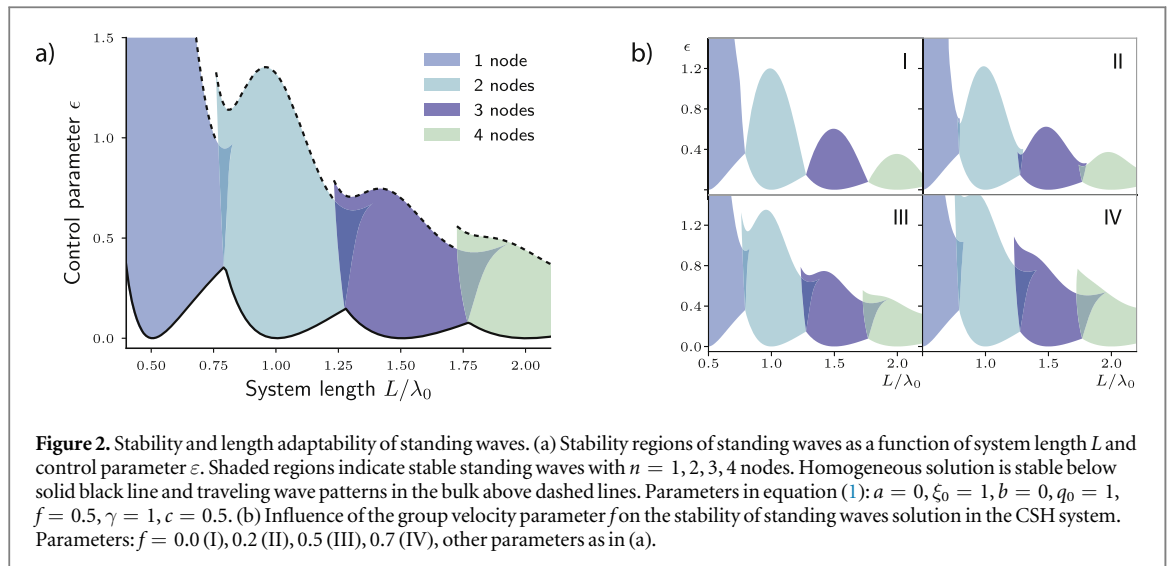
with amplitude F and frequency Ω ,

$$F^2 = \frac{1}{3\gamma}[\varepsilon - \xi_0^2(q_0^2 - q^2)^2], \quad (3)$$

$$\Omega = \frac{1}{\tau_0}[-a + \xi_0^2 b(q_0^2 - q^2)^2 + fq^2 + 3\gamma cF^2]. \quad (4)$$

Due to the no-flux boundaries, the wavenumber q is connected to the system length L via $q = n\pi/L$, where $n = 1, 2, 3 \dots$ is the number of nodes. This standing wave solution in equation (2) theoretically exists for $F^2 > 0$, i.e. for $\varepsilon > \xi_0^2(q_0^2 - q^2)^2$. In nature, e.g. in (bio)chemical reactions, the control parameter value, corresponding to ε in our model, is often fixed above the threshold of pattern formation. Then, standing waves only fulfill the aforementioned existence condition within a finite range of system lengths. Therefore standing waves with n nodes only exist in a certain length regime (existence band), located around $L = n\lambda_0/2$. In addition, existence ranges of standing waves with different numbers of nodes may overlap. Thus, for certain system lengths, multiple standing wave solutions (with different numbers of nodes) exist simultaneously. However, parameter ranges where patterns theoretically exist are not equivalent to the parameter ranges where they are stable. In fact, patterns are usually not stable throughout their whole existence range [3, 17, 27, 39–42]. By also analyzing the stability of standing waves, we thus identify the range in which to expect these solutions, especially in experiments (see SM is available online at stacks.iop.org/NJP/20/072001/mmedia for more details on the linear stability analysis).

Figure 2(a) shows the stability regions of standing wave solutions as a function of both system length L and the control parameter ε . For a given system length, standing waves with n nodes only exist for sufficiently large $\varepsilon > \xi_0^2(q_0^2 - (n\pi/L)^2)^2$. Below this threshold (black line in figure 2(a)), the homogeneous solution $u = 0$ is stable and no pattern occurs. The stability range of standing waves with n nodes is located around $L = n\lambda_0/2$ at

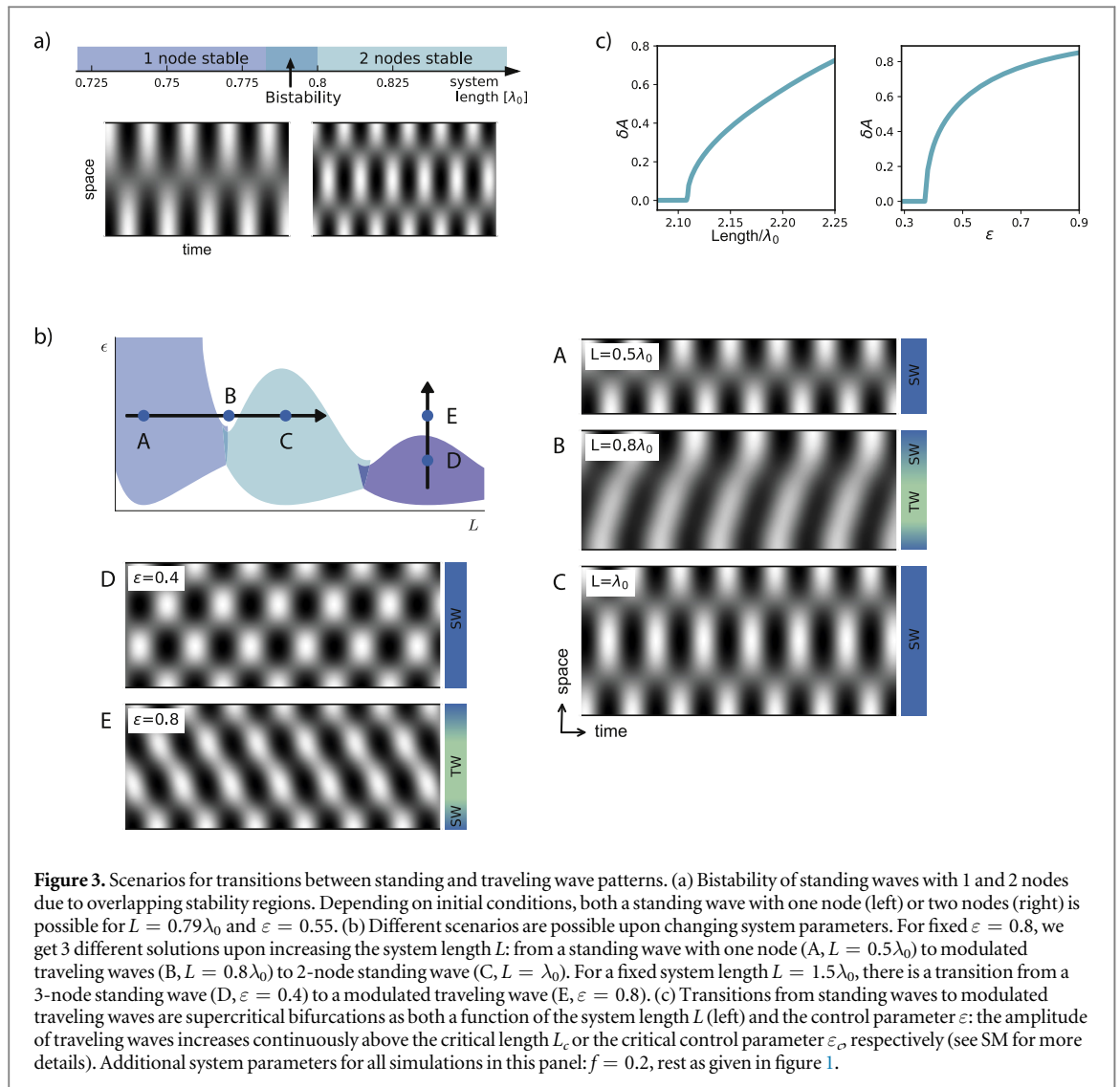


moderate values of ϵ . For $L = n\lambda_0/2$, the wavelength of the standing wave corresponds to the preferred wavelength λ_0 of the CSH model. For these ‘optimal’ system lengths, standing waves are stable over a large range of control parameter values. Nevertheless, we can deviate from these optimal lengths while still maintaining stable standing waves. This creates regions of stability in the ϵ - L -plane. These stability regions constitute the Eckhaus stability band for different number of nodes. We can now compare the width of the Eckhaus band to the width of the existence band for the standing waves. In extended systems, the waves are only stable in a subrange of their existence band. In contrast, in our confined systems close to the onset of pattern formation, the Eckhaus band spans the whole existence range (see figure 1 in SI). Additionally, adjacent stability regions may be large enough to overlap. In these cases, standing waves with both n and $n + 1$ nodes are stable. These overlapping stability regions therefore constitute areas of multistability. For large values of ϵ (above the dashed line in figure 2(a)), standing waves eventually lose stability. Simulations then show a transition to traveling wave patterns such as in figure 1 (top). The details of the stability regions also depend on the other parameters of the CSH model. Parameter f , e.g., which is connected to the group velocity of the waves, qualitatively changes the exact shape of the stability regions (figure 2(b)). As a result, the overlap between adjacent stability regions increases with increasing f . Other system parameters such as b or c only marginally change the stability of standing waves (figures S2 and S3) in confined systems. Importantly, however, the generic principle of a transition from traveling to standing waves in short systems remains qualitatively independent from system details.

Note that due to the shape of the stability regions, different scenarios are possible upon observing systems with increasing length: if we choose ϵ such that stability regions overlap, we expect direct transitions between standing waves with an increasing number of nodes (as seen in figure 1). Inside the overlap, there is bistability of standing waves with different numbers of nodes. Therefore, both types of standing waves are possible and the resulting pattern depends on initial conditions (see figure 3(a)). Notably, this provides the possibility for hysteresis. The transition from one to two nodes in a growing system, e.g., takes place at a different system length than the reverse transition in a shrinking system. For other values of ϵ , the different standing wave solutions are intersected by either the homogeneous solution (for small ϵ) or by traveling wave patterns (for larger ϵ , figures 3(b), (A)–(C)). In all cases, standing waves eventually lose stability for sufficiently large systems (after crossing the dashed line in figure 2(a)). For a fixed system length L , standing waves also lose their stability for sufficiently large ϵ (figures 3(b), (D)–(E)). These transitions to modulated traveling waves—both as a function of L and ϵ —take place in the form of supercritical (continuous) bifurcations (figure 3(c), see SM for details on how this was calculated).

4. Reflection-induced standing waves in models for a chemical reaction and the Min protein system

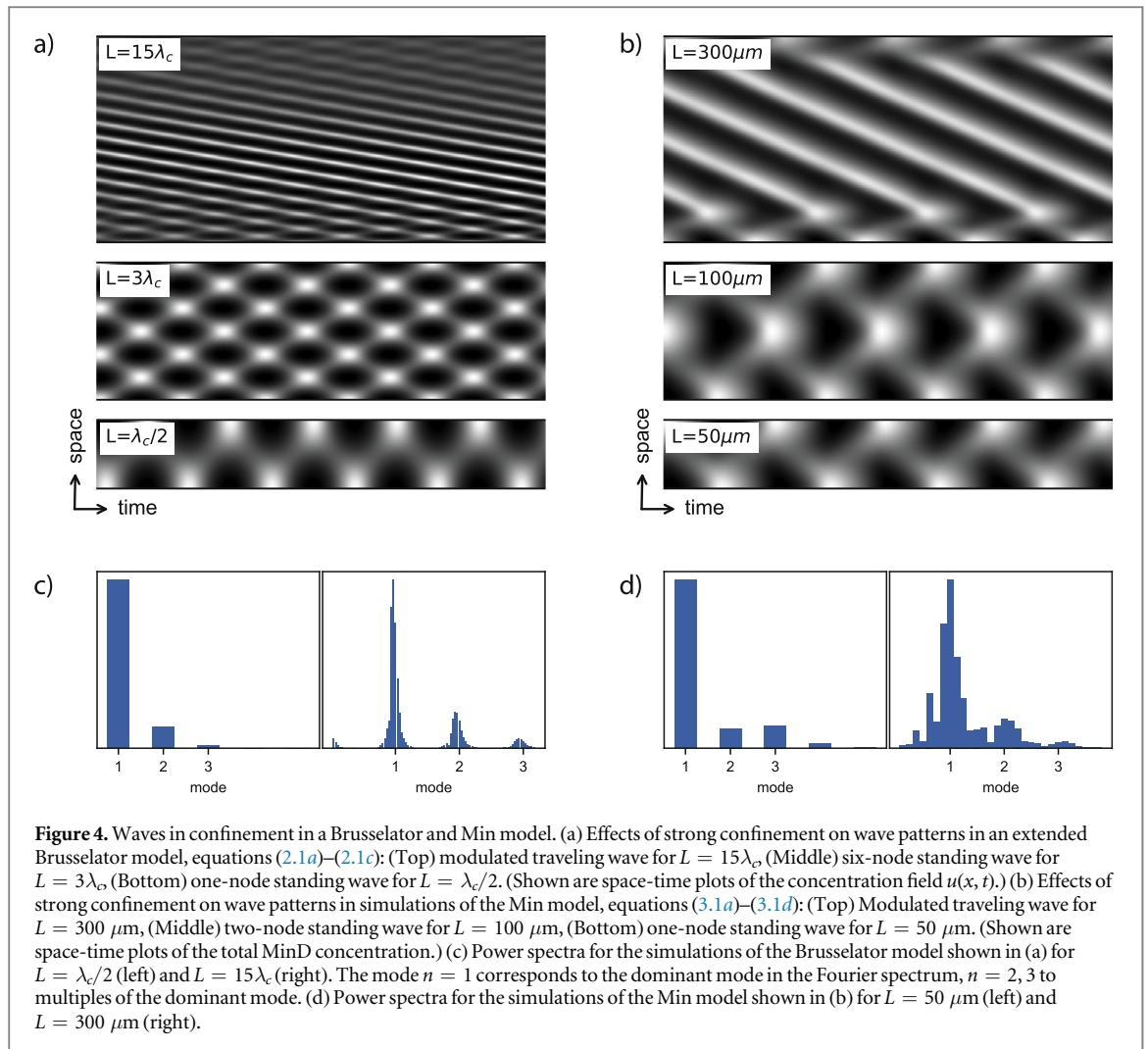
Minimal models such as the CSH model we study here for traveling waves are powerful tools to study system-spanning properties of self-organized patterns. System-specific models describing traveling waves are usually more complex than the CSH model. They are, e.g., often composed of several coupled nonlinear equations and/or include higher order nonlinearities (see e.g. [3, 21, 22, 44–49]). Moreover, traveling waves can occur far from the onset of pattern formation. Possible intricacies in these cases include secondary instabilities or anharmonic



wave profiles. Such effects can potentially overshadow the generic behavior of traveling waves under constraints discussed so far. Apart from these exceptions, however, even more complex scenarios often qualitatively follow generic principles extracted from minimal models. Thus, our results obtained from the generic CSH model help us to understand wave patterns in more complex systems.

We support this view by investigating the behavior of nonlinear traveling waves under confinement in two specific systems far from equilibrium. The first model describes the aforementioned Min protein oscillations in *E. coli* bacteria [21]. The second example is an extended Brusselator—a chemical reaction–diffusion model that forms traveling waves [49] (see appendices B and C for details on both models). As figures 4(a) and (b) show, the qualitative behavior of nonlinear waves in both of these models is very similar to the generic CSH model: in sufficiently strong confinement, traveling wave patterns inevitably change into reflection-induced standing waves. Depending on the system length, we also find standing wave patterns with different numbers of nodes. Note that both sets of simulations take place far beyond threshold. In this highly nonlinear regime the spatial dependence of the waves cannot be described by a single harmonic as in equation (2). Instead, they include higher harmonics—as seen in the Fourier spectra in figures 4(c) and (d).

Both models have a similar growth dispersion relation for perturbations of the homogeneous basic state as the CSH model—with a maximum at a finite wavenumber, while other modes are damped. Furthermore, the extended Brusselator shows a continuous bifurcation from the homogeneous state to traveling wave patterns—again, similar to the CSH model. On the basis of these common properties, the similar behavior of nonlinear waves in strong confinement were to be expected. Traveling waves in the Min model in figure 4(b) are even further from threshold and thus in the strongly nonlinear regime. Nevertheless, we find the same scenarios for the Min reaction as for the CSH model and the Brusselator. This further supports the generic nature of our predictions on reflection-induced standing waves.



Furthermore, our findings are not limited to no-flux boundary conditions. The reflection-induced transition to standing waves prevails for different boundary conditions such as fixed boundaries ($u|_{x=0} = u|_{x=L} = 0$). The only qualitative difference is the position of the standing wave nodes: they are shifted to the boundaries due to the vanishing fields at these points (see figure S4).

Nonlinear traveling waves in extended systems may be convectively unstable directly beyond threshold. This is also known as Benjamin–Feir instability [3, 4]. For the CSH model, this is the case in the parameter range $(b + f/4\xi_0^2 q_0^2)c > -1$. In this Benjamin–Feir unstable regime, spatio-temporally chaotic solutions are possible (above the transition to absolute instability). System size matters for spatio-temporal chaos as well: strong confinement and the related boundary-induced reflection can reestablish ordered standing waves (see figure S5).

5. Discussion

In our work we identified generic properties of nonlinear waves in very short systems, i.e. under strong spatial confinement. We found a universal and robust reflection-induced transition from traveling wave patterns in extended systems to standing waves in sufficiently short systems. Stability analysis shows that these standing waves can adapt to different system lengths. This corresponds to stability within a finite wavenumber band—a feature they share with stationary spatially periodic patterns or traveling waves [3, 17, 38–42]. They can also react to larger length variations by changing their number of nodes. We also find multistability of standing waves with different numbers of nodes in a system of the same length.

Our results obtained in terms of basic pattern formation theory show striking similarities to oscillating Min protein patterns. We hypothesize that basic generic properties of nonlinear wave patterns have a key function in the Min system. They may provide the missing link between pole-to-pole Min oscillations in short systems [31, 50–52] and traveling protein waves on extended membranes [21, 22]: the pole-to-pole oscillations in *E. coli* behave like standing waves originating from traveling waves confined to short systems. We also suggest that generic features of the reflection-induced standing waves such as length adaptability further contribute to the

regulation of cell division. This view is supported by experimental observations in the Min system: depending on bacteria length, the Min proteins also form standing waves with multiple nodes [31, 47, 53] or even traveling waves [47]. More importantly though, not only do living bacteria slightly differ in length, they also actively grow. To maintain accurate cell division at the cell center, the pole-to-pole oscillations must be robust over a range of cell sizes. The generic length adaptability of reflection-induced standing waves enables pole-to-pole oscillations in the Min system to adapt to the growing cell. In fact, *E. coli* maintain robust pole-to-pole oscillations even as they almost double in length prior to cell division. Continued cell growth to filamentous bacteria also allows for transitions between standing waves with different numbers of nodes or to traveling waves [33, 47, 53]. Even multistability of different wave patterns has recently been found in living *E. coli* [51].

Due to their generic nature, we expect our findings to be independent of system details. Our simulations of a Min protein model and an extended Brusselator substantiate this claim. While we analyzed one-dimensional systems in this work, we believe the basic principles also apply to two or three spatial dimensions: in sufficiently small multidimensional systems the boundary reflection of traveling waves along the long axis will likely overrule the bulk competition between counter-propagating traveling waves. Thus, system borders force them into reflection-induced standing waves—with slight system-specific modifications. Fluid experiments [17, 30] or oscillating chemical reactions guided by recent models as in [48, 49] are further suitable candidates to verify our results. Pattern formation theory applied to stationary 2d patterns recently provided important insights into pattern orientation with respect to spatial inhomogeneities or confinement [28, 54]. A combination of these approaches with our analysis of nonlinear traveling waves in confined systems is very promising. It may reveal further generic properties of nonlinear traveling waves and, e.g., provide additional guidance for experiments in 2d Min systems [50, 52]. This is particularly interesting for designing bottom-up approaches in synthetic biology to reconstitute cells [52]. In this context, our robust rules about nonlinear (protein) waves may present another puzzle piece to understand how nature controls crucial steps of life.

Acknowledgments

Support by the Elite Study Program Biological Physics is gratefully acknowledged.

Appendix A. Simulation methods

We solve the CSH model as well as the models for the Min oscillations and the chemical reactions below numerically by using a pseudo-spectral method with a semi-implicit time step (implicit Euler for the linear part of the equation, explicit Euler for the nonlinearities) (66). We calculate all spatial derivatives by transformation to a suitable function space depending on the boundary conditions. We use Fourier representations of the fields for periodic boundaries (i.e. in case of the CSH model $u|_{x=0} = u|_{x=L}$), a cosine transform for no-flux boundaries ($\partial_x u|_{x=0,L} = 0$) and a sine transform for vanishing fields at the boundary ($u|_{x=0,L} = 0$), where L is the system length.

Appendix B. Oscillating chemical reaction

As a model for a pattern forming chemical reaction, we use an extended Brusselator model as proposed by Yang *et al* [49]. The Brusselator is a well-known prototype for reaction–diffusion systems. Typically, this system is a two-component activator-inhibitor model with a bifurcation to Turing patterns or homogenous Hopf oscillations. The model by Yang *et al* extends the Brusselator by a third component. The dynamics of the three concentration fields u , v and w are given by:

$$\partial_t u = D_u \partial_x^2 u + a - (b + 1)u + u^2 v - cu + dw, \quad (2.1a)$$

$$\partial_t v = D_v \partial_x^2 v + bu - u^2 v, \quad (2.1b)$$

$$\partial_t w = D_w \partial_x^2 w + cu - dw. \quad (2.1c)$$

We choose $a = 0.8$, $c = 2$, $d = 1$, $D_u = 0.01$, $D_v = 0$ and $D_w = 1$. We consider b the control parameter of the system. The homogeneous solution ($u_h = a$, $v_h = b/a$, $w_h = ac/d$) becomes unstable towards traveling waves at the critical value $b_c = 3.076$. The intrinsic wavelength of the traveling wave pattern above threshold is $\lambda_c \approx 9.5$. We perform our simulations close to pattern onset, for $b = b_c(1 + \varepsilon)$ where $\varepsilon = 0.005$. The onset of the Turing instability (i.e. of stationary periodic patterns) tends to infinity for $D_v \rightarrow 0$. By choosing $D_v = 0$, we thereby eliminate any competition between traveling waves and Turing structures.

Appendix C. Min oscillation model

As a representative model for the Min oscillations shown in figure 4, we consider the model given by equations (3.1a)–(3.1d) as proposed by Loose *et al* [22] (see also equations [1]–[4] in their supplementary information). This model describes the dynamics of both MinD and MinE in the cytosol (c_D and c_E , respectively), the MinD concentration on the membrane c_d and the concentration of MinD/MinE complexes on the membrane c_{de} :

$$\partial_t c_D = D_D \partial_x^2 c_D + \omega_{de} c_{de} - c_D (\omega_D + \omega_{dD} c_d), \quad (3.1a)$$

$$\partial_t c_E = D_E \partial_x^2 c_E + \omega_{de} c_{de} - c_E c_d (\omega_E + \omega_{eE} c_{de}^2), \quad (3.1b)$$

$$\partial_t c_d = D_d \partial_x^2 c_d + c_D (\omega_D + \omega_{dD} c_d) - c_E c_d (\omega_E + \omega_{eE} c_{de}^2), \quad (3.1c)$$

$$\partial_t c_{de} = D_{de} \partial_x^2 c_{de} + c_E c_d (\omega_E + \omega_{eE} c_{de}^2) - \omega_{de} c_{de}. \quad (3.1d)$$

For the simulation shown in figure 4 we choose the parameters as suggested in [22]: $D_D = D_E = 60 \mu\text{m}^2 \text{s}^{-1}$, $D_d = 1.2 \mu\text{m}^2 \text{s}^{-1}$, $D_{de} = 0.4 \mu\text{m}^2 \text{s}^{-1}$, $\omega_{de} = 0.029 \text{s}^{-1}$, $\omega_D = 2.9 \cdot 10^{-4} \text{s}^{-1}$, $\omega_{dD} = 4.8 \cdot 10^{-8} \mu\text{m}^2 \text{s}^{-1}$, $\omega_E = 1.9 \cdot 10^{-9} \mu\text{m}^2 \text{s}^{-1}$, $\omega_{eE} = 2.1 \cdot 10^{-20} \mu\text{m}^6 \text{s}^{-1}$. We choose a total MinD concentration of $c_{D,\text{tot}} = c_D + c_d + c_{de} = 3.6 \cdot 10^6 \mu\text{m}^{-2}$, and a total MinE concentration of $c_{E,\text{tot}} = c_E + c_e + c_{de} = 5.8 \cdot 10^6 \mu\text{m}^{-2}$. In large, quasi-unconfined systems this leads to traveling waves with a typical wavelength $\lambda_{\text{min}} \approx 71 \mu\text{m}$.

References

- [1] Ball P 1998 *The Self-Made Tapestry: Pattern Formation in Nature* (Oxford: Oxford University Press)
- [2] Cross M C and Greenside H 2009 *Pattern Formation and Dynamics in Nonequilibrium Systems* (Cambridge: Cambridge University Press)
- [3] Cross M C and Hohenberg P C 1993 Pattern formation outside of equilibrium *Rev. Mod. Phys.* **65** 851
- [4] Aranson I and Kramer L 2002 The world of the complex Ginzburg–Landau equation *Rev. Mod. Phys.* **74** 99
- [5] Kondo S and Miura T 2010 Reaction–diffusion model as a framework for understanding biological pattern formation *Science* **329** 1616
- [6] Lander A D 2011 Pattern, growth, and control *Cell* **144** 955
- [7] Murray S M and Sourjik V 2017 Self-organization and positioning of bacterial protein clusters *Nat. Phys.* **13** 1006
- [8] Sasai Y 2013 Cytosystems dynamics in self-organization of tissue architecture *Nature* **493** 318
- [9] Kondo S and Asai R 1995 A reaction–diffusion wave on the skin of the marine angelfish *Pomacanthus* *Nature* **376** 786
- [10] Singh A P and Nüsslein-Volhard C 2015 Zebrafish stripes as a model for vertebrate colour pattern formation *Curr. Biol.* **25** R81
- [11] Lappa M 2009 *Thermal Convection: Patterns, Evolution and Stability* (New York: Wiley)
- [12] Meron E 2015 *Nonlinear Physics of Ecosystems* (Boca Raton, FL: CRC Press)
- [13] Meron E 2012 Pattern-formation approach to modelling spatially extended ecosystems *Ecol. Modelling* **234** 70
- [14] Getzin S, Yizhaq H, Bell B, Erickson T E, Postle A, Katra I, Tzuk O, Zelnik Y R, Wiegand K and Meron E 2016 Discovery of fairy circles in australia supports self-organization theory *Proc. Natl Acad. Sci. USA* **113** 3551
- [15] Moses E, Fineberg J and Steinberg V 1987 Multistability and confined traveling-wave patterns in a convecting binary mixture *Phys. Rev. A* **35** 2757
- [16] Heinrichs R, Ahlers G and Cannell D S 1987 Traveling waves and spatial variation in the convection of a binary mixture *Phys. Rev. A* **35** 2761
- [17] Kolodner P 1992 Extended states of nonlinear traveling-wave convection. I. The Eckhaus instability *Phys. Rev. A* **46** 6431
- [18] Schöpf W and Zimmermann W 1993 Convection in binary fluids: amplitude equations, codimension-2 bifurcation, and thermal fluctuations *Phys. Rev. E* **47** 1739
- [19] Rehberg I, Rasenat S, Fineberg J, de la Torre Juárez M and Steinberg V 1988 Temporal modulation of traveling waves *Phys. Rev. Lett.* **61** 2449
- [20] Kramer L and Pesch W 1995 Convection instabilities in nematic liquid crystals *Annu. Rev. Fluid Mech.* **27** 515
- [21] Loose M, Fischer-Friedrich E, Ries J, Kruse K and Schwille P 2008 Spatial regulators for bacterial cell division self-organize into surface waves *in vitro Science* **320** 789
- [22] Schweizer J, Loose M, Bonny M, Kruse K, Mönch I and Schwille P 2012 Geometry sensing by self-organized protein patterns *Proc. Natl Acad. Sci. USA* **109** 15283
- [23] Cross M C 1982 Boundary conditions on the envelope function of convective rolls close to onset *Phys. Fluids* **25** 936
- [24] Kramer L and Hohenberg P C 1984 Effects of boundaries on periodic structures *Physica D* **13** 352
- [25] Greenside H S and Coughran W M 1984 Nonlinear pattern formation near the onset of Rayleigh–Bénard convection *Phys. Rev. A* **30** 398
- [26] Kramer L, Ben-Jacob E, Brand H and Cross M C 1982 Wavelength selection in systems far from equilibrium *Phys. Rev. Lett.* **49** 1891
- [27] Riecke H and Paap H G 1986 Stability and wave-vector restriction of axisymmetric Taylor vortex flow *Phys. Rev. A* **33** 547
- [28] Rapp L, Bergmann F and Zimmermann W 2016 Pattern orientation in finite domains without boundaries *Europhys. Lett.* **113** 28006
- [29] Cross M C 1988 Structure of nonlinear traveling-wave states in finite geometries *Phys. Rev. A* **38** 3593
- [30] Garnier N, Chiffaudel A and Daviaud F 2003 Nonlinear dynamics of waves and modulated waves in 1d thermocapillary flows. II. convective/absolute transitions *Physica D* **174** 30
- [31] Raskin D M and de Boer P A J 1999 Rapid pole-to-pole oscillation of a protein required for directing division to the middle of *Escherichia coli* *Proc. Natl Acad. Sci. USA* **96** 4971
- [32] Lutkenhaus J 2007 Assembly dynamics of the bacterial MinCDE system and spatial regulation of the Z ring *Annu. Rev. Biochem.* **76** 539
- [33] Loose M, Kruse K and Schwille P 2011 Protein self-organization: lessons from the min system *Annu. Rev. Biophys.* **40** 315
- [34] Malomed B A 1984 Nonlinear waves in nonequilibrium systems of the oscillatory type, part I *Physik B* **55** 241
- [35] Aranson I and Tsimring L 1995 Domain walls in wave patterns *Phys. Rev. Lett.* **75** 3273

- [36] Gelens L and Knobloch E 2011 Traveling waves and defects in the complex Swift–Hohenberg equation *Phys. Rev. E* **84** 056203
- [37] Eckhaus V 1965 *Studies in Nonlinear Stability Theory* (Berlin: Springer)
- [38] Kramer L and Zimmermann W 1985 On the Eckhaus instability for spatially periodic patterns *Physica D* **16** 221
- [39] Lowe M and Gollub J P 1985 Pattern selection near the onset of convection: the Eckhaus instability *Phys. Rev. Lett.* **55** 2575
- [40] Dominguez-Lerma M A, Cannell D S and Ahlers G 1986 Eckhaus boundary and wave-number selection in rotating Couette–Taylor flow *Phys. Rev. A* **34** 4956
- [41] Zimmermann W and Kramer L 1985 Wavenumber restriction in the buckling instability of a rectangular plate *J. Phys.* **46** 343
- [42] Janiaud B, Pumir A, Bensimon D, Croquette V, Richter H and Kramer L 1992 The Eckhaus instability for traveling waves *Physica D* **55** 269
- [43] Liu Y and Ecke R E 1997 Eckhaus–Benjamin–Feir instability of rotating convection *Phys. Rev. Lett.* **78** 4391
- [44] Howard M, Rutenberg A D and de Vet S 2001 Dynamic compartmentalization of bacteria: accurate division in *E. coli* *Phys. Rev. Lett.* **87** 278102
- [45] Meinhardt H and de Boer P A J 2001 Pattern formation in *Escherichia coli*: a model for the pole-to-pole oscillations of Min proteins and the localization of the division site *Proc. Natl Acad. Sci. USA* **98** 14202
- [46] Halatek J and Frey E 2012 Highly canalized MinD transfer and MinE sequestration explain the origin of robust MinCDE-protein dynamics *Cell Reports* **1** 741
- [47] Bonny M, Fischer-Friedrich E, Loose M, Schwille P and Kruse K 2013 Membrane binding of MinE allows for a comprehensive description of min-protein pattern formation *PLoS Comput. Biol.* **9** e1003347
- [48] Bánsági T, Vanag V K and Epstein I R 2012 Two- and three-dimensional standing waves in a reaction–diffusion system *Phys. Rev. E* **86** 045202
- [49] Yang L, Dolnik M, Zhabotinsky A M and Epstein I R 2002 Pattern formation arising from interactions between Turing and wave instabilities *J. Chem. Phys.* **117** 7259
- [50] Wu F, van Schie B G C, Keymer J E and Dekker C 2015 Symmetry and scale orient Min protein patterns in shaped bacterial sculptures *Nat. Nanotechnol.* **10** 719
- [51] Wu F, Halatek J, Reiter M, Kingma E, Frey E and Dekker C 2016 Multistability and dynamic transitions of intracellular protein patterns *Mol. Syst. Biol.* **12** 873
- [52] Zieske K and Schwille P 2014 Reconstitution of self-organized protein gradients as spatial cues in cell-free systems *eLife* **3** e03949
- [53] Fischer-Friedrich E, Meacci G, Lutkenhaus J, Chaté H and Kruse K 2010 Intra- and intercellular fluctuations in Min-protein dynamics decrease with cell length *Proc. Natl Acad. Sci. USA* **107** 6134
- [54] Hiscock T W and Megason S G 2015 Orientation of Turing-like patterns by Morphogen gradients tissue anisotropies *Cell Syst.* **1** 408